Effect of Buffer on Kinetics of Proton Equilibration with a Protonable Group†

Menachem Gutman,* Esther Nachliel, and Eli Gershon
Department of Biochemistry, Tel Aviv University, Tel Aviv, Israel
Received June 22, 1984; Revised Manuscript Received November 2, 1984

ABSTRACT: The laser-induced proton pulse generates a massive, brief, proton pulse capable of perturbing biochemical equilibria. The time resolution of the monitoring system can follow the diffusion-controlled protonation of specific sites on macromolecular bodies [Gutman, M. (1984) *Methods Biochem. Anal. 30*, 1–103]. In order to apply this method in enzymology, one must first evaluate how the buffer capacity of biochemical systems (substrates and proteins) will affect the observed dynamics. Unlike equilibrium measurements, where buffer is an inert component, in kinetic studies buffer modulates the observed dynamics. In this paper we analyze the effect of buffer on the dynamics of protonation in a model system. We describe the experimental technique and introduce the mathematical formalism that determines the various rate constants involved in the reaction. The analysis of the experiments indicates that in buffered solution proton flux is carried by two mechanisms: (A) proton dissociation followed by free proton diffusion; (B) collisional proton transfer between small diffusing solutes. We demonstrate how to evaluate the contribution of each pathway to the overall proton flux.

Proteins are polyelectrolytes carrying many titrable groups. During successive protonation the molecular charge is changed with a subsequent shift of the equilibrium constants. This complex interdependence has been analyzed by Tanford & Kirkwood's (1957) electrostatic theory, as demonstrated by the studies of Shire et al. (1974a,b, 1975), Tanford (1976), Mathew et al. (1981), and March et al. (1982). While the equilibration of proton with protein is well-known, the dynamics of this reaction has never been studied at the time scale of the elementary molecular event, the association of the proton with the conjugate bases on the protein. These events are diffusion-controlled second-order reactions with rate constants too fast to be studied by conventional methods. In most cases, the kinetic studies of protein protonation were limited to the secondary events like conformation changes (June et al., 1981), ligand binding (MacKnight et al., 1973), proton release during catalysis (Bennett et al., 1982), or redox changes (Silvestrini et al., 1981; Corin et al., 1983).

To measure the rate of protonation of a specific site on an enzyme, we have first to evaluate how the buffering capacity of the protein modulates the observed dynamics. In equilibrium studies the buffer is an inert component and does not affect the pK of the titrated group. In kinetic studies the buffer competes for the protons, altering all measurable parameters. If we wish to analyze the kinetics of protonation of a specific site on a protein, we must first understand the kinetic role of the buffer.

The laser-induced proton pulse (Gutman & Huppert, 1979) has the time resolution and analytic capacity suitable to measure the diffusion-controlled protonation of small solutes (Gutman et al., 1981, 1983b) or of specific sites on macromolecules (Gutman et al., 1983b; Nachliel & Gutman, 1984). For review, see Gutman (1984). In this study we apply this method for analyzing the reactions taking place in a buffered solution. We demonstrate how the differential rate equations are solved and through them explain the manifold effect of buffer on the observed parameters. In the accompanying paper (Gutman & Nachliel, 1985) we shall expand our previous studies (Nachliel & Gutman, 1984) to formulate a comprehensive model for the dynamics of protonation of a specific site on self-buffered macromolecular bodies.

† This research was supported by the American–Israel Binational Science Foundation, 3101/82.

Materials and Methods

Materials. 8-Hydroxypyrene-1,3,6-trisulfonate (laser grade, Eastman) and bromocresol green (Sigma) were used without further purification. 2-Naphthol-3,6-disulfonate and imidazole were recrystallized before use.

Methods. Transient absorbancies of the pulsed solution were monitored by either HeCd (441 nm) or HeNe (633 nm) CW lasers as a probing light source. The excitation pulse (5 mJ, 10 ns full width at half maximum, 337.4 nm) of a Molectron UV-14 nitrogen laser was focused at one side of a four-face quartz cuvette (10 mm × 10 mm) to give a homogeneously illuminated horizontal rectangle with dimensions of 15 mm × 4 mm. The solution illuminated by this beam was probed by the monitoring light. The probing beam, parallel with the face fronting the excitation pulse, passed 1 mm behind the excited surface of the cuvette (Gutman, 1984). The signals of the photomultiplier were recorded by a Biomation 8100 transient recorder and stored by a Nicolet 1170 signal averager. All the measured or calculated transients are expressed in molar units.

Results

Effect of Buffer on Dynamics of Protonation. In its ground state, the proton emitter 8-hydroxypyrenetrisulfonate has two absorption bands. The neutral form (ROH) has λ_{max} = 400 nm while for the anionic form (RO^-) λ_{max} = 445 nm. Excitation of ROH by a short laser pulse initiates a transient dissociation of ROH that is measured as incremental absorption of 441 nm. The presence of buffer in the reaction system modulates both the amplitude of the signal and its relaxation dynamics (Figure 1).

Kinetic Analysis of Relaxation in the Presence of Buffer. The reactions taking place in the perturbed sample are the dissociation of the proton emitter, the dissociation of the buffer, and a direct proton exchange between them (reactions 1–3, respectively).

0006-2960/85/0424-2937$01.50/0

$$ROH \underset{k_2}{\overset{k_1}{\rightleftharpoons}} RO^- + H^+ \quad (1)$$

$$BH \underset{k_6}{\overset{k_5}{\rightleftharpoons}} B^- + H^+ \quad (2)$$

$$BH + RO^- \underset{k_{10}}{\overset{k_9}{\rightleftharpoons}} B^- + ROH \quad (3)$$

The pulse excitation of the emitter leads to an incremental dissociation of ROH—defined as X_0. The discharged protons react with Z molecules of B^-; thus the increment of free protons is given by $[H^+]_t = X_t - Z_t$. The perturbation relaxes by the dissociation of the species followed by proton diffusion and, in parallel, direct collision between the reactants (reaction 3).

The differential rate equations describing the relaxation are given in eq 4 and 5, where [A] represents the equilibrium concentration of component A.

$$dx/dt = -[k_1([RO^-] + [H^+]) + k_2 + k_{10}[BH] - k_9[B^-]]X + (k_1[RO^-] - k_{10}[RO^-] - k_9[ROH])Z - k_1X^2 + (k_1 - k_{10} + k_9)XZ \quad (4)$$

$$dz/dt = (k_5[B^-] - k_9[B^-] - k_{10}[BH])X - [k_5([B^-] + [H^+]) + k_6[ROH] + k_{10}[RO^-]]Z + k_5Z^2 + (k_9 - k_5 - k_{10})XZ \quad (5)$$

At pH 7 and in the presence of high reactant concentrations, one may assume that the reaction proceeds mostly through the direct proton exchange (reaction 3). Under such approximations, the time constant of the relaxation is given by a simple expression (Eigen, 1964; Czerlinsky, 1966):

$$\gamma_2 = k_{10}([RO^-] + [BH]) + k_9([ROH] + [B^-]) \quad (6)$$

A plot of $\gamma_2/([RO^-] + [BH])$ vs. $([ROH] + [B^-])/([RO^-] + [BH])$ gives a straight line with a slope of $k_9 = 7 \times 10^8$ M^{-1} s^{-1} and intercept of $k_{10} = 2 \times 10^9$ M^{-1} s^{-1} (Figure 2).

The equilibrium constant for reaction 3 as derived from our kinetic analysis is $K_{10,9} = 23 \pm 3$ while from the measured pK of the reactants we obtain $K_{10,9} = K_{6,5}/K_{2,1} = 5.0$. This discrepancy indicates that the contribution of proton diffusion cannot be ignored even when its concentration is so small: $[H^+] = 10^{-7}$ M.

Equations 4 and 5 are solved numerically as nonlinear parametric coupled differential equations. Of the six rate constants defined in eq 1–3, two are already known (k_1 and k_2) (Gutman et al., 1983b), while the equilibrium constants $K_{6,5}$ and $K_{10,9}$ reduce the number of unknown rate constants to two: k_5 and k_{10}. The solution for the parametric differential equations (reactions 4 and 5) will be a pair of rate constants, (k_5, k_{10}), which will generate a function with amplitude and relaxation time (γ_2) compatible with the experimentally measured one.

Figure 3A depicts the variation of γ_2, as calculated by the differential equation, as function of k_5 for four values of k_{10}. Figure 3B represents γ_2 dependence on k_{10} for three values of k_5. The dotted lines denote γ_2 as measured. The combination of k_{10} and k_5 that will set values between the two dotted lines is a legitimate solution. As seen from this figure only the combination $k_5 = (2.2 \pm 0.4) \times 10^{10}$ M^{-1} s^{-1} and $k_{10} = (2.5 \pm 0.5) \times 10^9$ M^{-1} s^{-1} satisfies these demands.

The accuracy of the solution is demonstrated in Figure 4. This figure relates the dependence of γ_2 on the initial conditions of the reaction. It depicts the results of two sets of experiments, carried out in the absence or the presence of 2 mM imidazole. In the absence of buffer the relaxation is accelerated by increasing the prepulse pH. In the presence of buffer the relaxation is slowed at higher pH values. The

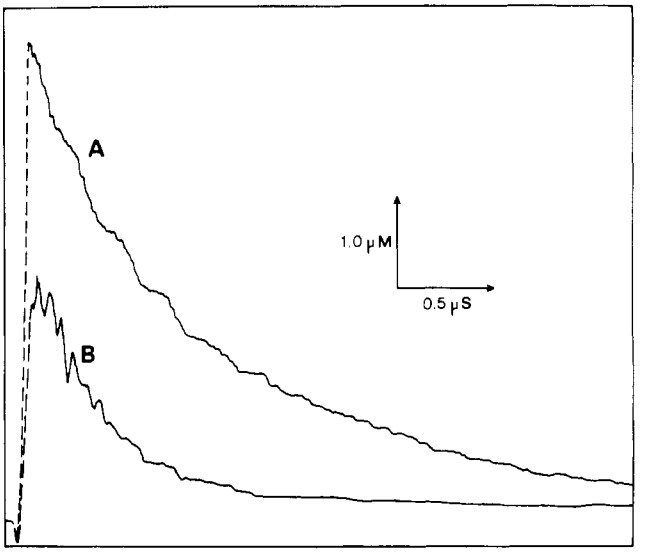

FIGURE 1: Transient absorption of 8-hydroxypyrene-1,3,6-trisulfonate following pulse excitation. The emitter solution (100 μM) was excited by 10-ns pulses of nitrogen laser (λ = 337 nm) at a repetition rate of 15 Hz. The energy density of the excitation pulse was 0.15 M W cm^{-2}. The concentration of the ground-state anion was monitored through its enhanced observation at 441 nm ($\epsilon_{441} = 24 \times 10^3$ M^{-1} cm^{-1}), using a CW HeCd laser as a light source. The data were collected with a Biomation 8100 transient recorder at 10 ns/address and accumulated by a Nicolet 1170 signal averager (512 events). The signal amplitude is calibrated in micromolar units. (Line A) No buffer present, pH 6.95; (line B) 2 mM imidazole, pH 7.46, present in the pulsed solution.

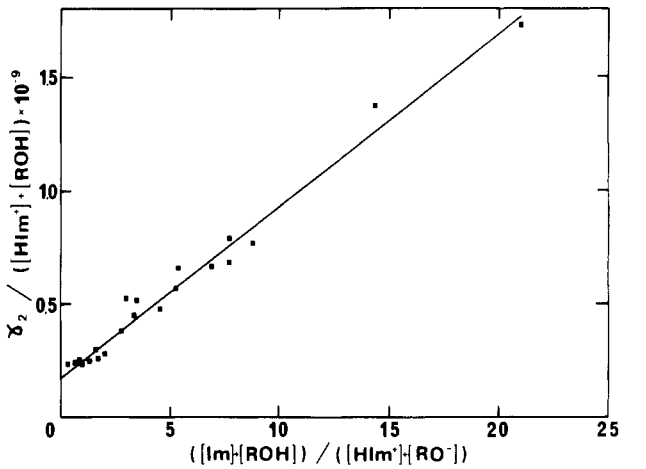

FIGURE 2: Effect of buffer on the rate of trisulfonopyrenate reprotonation. The rate constant of relaxation (γ_2) was measured from experiments, as in Figure 1, carried out at varying imidazole concentrations of 0.1–10 mM and pH 6.5–8.5. The results are presented according to eq 6.

two lines drawn through the experimental points are theoretically computed, with the rate constants listed in Table I.

Effect of Buffer on Dynamics of Protonation of an Indicator. The reactions taking place in a three-component system consisting of proton emitter, indicator, and buffer are

$$ROH \underset{k_2}{\overset{k_1}{\rightleftharpoons}} RO^- + H^+ \quad (7)$$

$$HIn \underset{k_4}{\overset{k_3}{\rightleftharpoons}} In^- + H^+ \quad (8)$$

$$BH \underset{k_6}{\overset{k_5}{\rightleftharpoons}} B^- + H^+ \quad (9)$$

$$BH + In^- \underset{k_8}{\overset{k_7}{\rightleftharpoons}} HIn + B^- \quad (10)$$

$$BH + RO^- \underset{k_{10}}{\overset{k_9}{\rightleftharpoons}} B^- + ROH \quad (11)$$

$$RO^- + HIn \underset{k_{12}}{\overset{k_{11}}{\rightleftharpoons}} ROH + In^- \quad (12)$$

The corresponding differential rate equations describing the deviation of RO^- (X), HIn (Y), and BH (Z) from their equilibrium concentration are given in the Appendix. An experimental curve and the function generated by the numerical solution of the equations are demonstrated in Figure 5. A list of the various rate constants calculated from measurements carried out with different imidazole concentrations and two proton emitters is given in Table I.

Discussion

The dynamics of protonation of specific targets in a buffered solution can be analyzed at several levels of complexity and precision. The simplest analysis is according to Eigen's (1964) approximation, valid when buffer concentration is high and pH is close to 7. As demonstrated under Results, this approximative solution introduces a small, but nonnegligible systematic error. In a case where one is looking for better values, those obtained by this approximation are used as the estimated magnitude of the rate constant for the rigorous numerical solution of the relaxation equations (eq 4 and 5).

The dynamics of pulse protonation is dominated by two types of reaction mechanisms, the competition of all present bases (RO^-, In^-, and B^-) for the protons and the direct proton exchange between each acid with the other conjugate bases (Gutman et al., 1983; Gutman, 1984). These reactions explain the manifold effects of the buffer on the observed dynamics.

As seen in Figure 4, the protonation of RO^- is accelerated at low pH in the presence of buffer, while in its absence we observe a small deceleration of the relaxation. In the absence of buffer, the only reactants present are ROH, RO^-, and H^+. When the pH of such a system approaches the pK of the proton emitter, the prepulse concentration of RO^- increases, with consequent faster trapping of the discharged protons by RO^-. In the presence of buffer, the relaxation below pH 7 is faster than that in the absence of buffer. This is due to increasing concentration of H^+–imidazole serving as a proton donor to the negatively charged sulfonopyrenate. At pH values higher than the buffer's pK, the increased [imidazole] fraction in the solution is competing effectively for the protons, while the diminished H^+–imidazole concentration cannot protonate the RO^-. The combination of the two effects prolongs the relaxation of the system. Indeed, at pH 8 the relaxation in the absence of buffer is faster than in its presence.

The numerical solution of the differential rate equations can reconstruct the dynamics of all participating reactants—not only that of the observed one (the indicator). This advantage is represented in Figure 6, which simulates the dynamics of the emitter, detector, free protons, and buffer in a system consisting of 2-naphtholdisulfonate, bromocresol green, and imidazole.

Figure 6 (BH^+) depicts the simulated dynamics of imidazole at pH 6, 7, and 8. At pH 6, about 90% of the buffer is in the form H^+–imidazole. When the equal amounts of H^+ and RO^- are generated by the laser pulse, the collisional deprotonation of [H^+–imidazole] by RO^- will be faster than the protonation of the small fraction of the conjugate base:

$$k_5[B][H^+] < k_9[BH^+][RO^-] \quad (13)$$

Subsequently, the net change in H^+–imidazole concentration at pH 6 is negative. At higher pH values, the increasing ratio B/BH^+ will change the magnitude of the left and right terms in expression 13, reversing the sign of inequality. Indeed at pH 7 and 8 the transient of [H^+–imidazole] is positive. [For precise analysis, see Gutman et al. (1983b).]

A similar scenario is observed in the dynamics of RO^- [Figure 6 (RO^-)]. The protonation of RO^- at pH 6 is faster

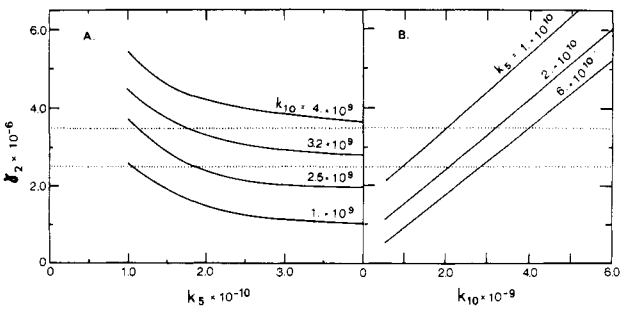

FIGURE 3: Dependence of the computed relaxation of trisulfonopyrenate on the rate constants of buffer protonation (k_5) and proton transfer from buffer to emitter anion (k_{10}). The lines drawn are computer-generated dependencies on the two parameters as obtained by numerical solution of eq 4 and 5 with $k_1 = 1.6 \times 10^{11}$ M^{-1} s^{-1}, $pK_{2,1} = 7.7$, and the experimental concentrations of reactants corresponding to those of line B in Figure 1. The dotted lines denote the upper and lower values of the experimentally measured γ_2.

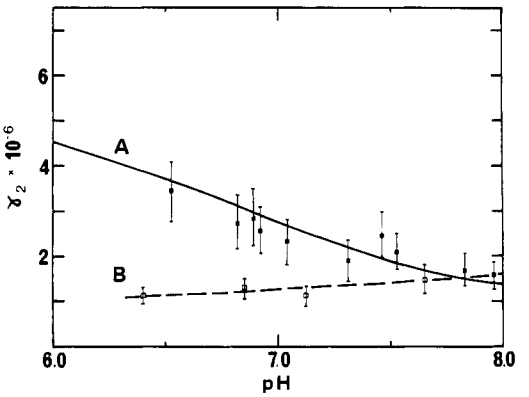

FIGURE 4: Effect of pH on the rate of reprotonation of trisulfonopyrenate following laser-induced proton dissociation. The reaction was measured as in Figure 1 in the presence of 2 r imidazole (line A) or in the absence of buffer (line B). The continuous lines are computed for curves generated by the numerical solution of the differential rate equations (eq 4 and 5) with the parameters $k_1 = 1.6 \times 10^{11}$ M^{-1} s^{-1}, $k_5 = 3.5 \times 10^{10}$ M^{-1} s^{-1}, and $k_{10} = 2.1 \times 10^{10}$ M^{-1} s^{-1}.

Table I: Rate Constants of Reactions between Proton Emitter, Bromocresol Green, and Imidazole[a]

rate constant (M^{-1} s^{-1})	8-hydroxypyrene-1,3,6-trisulfonate (M^{-1} s^{-1})	2-naphthol-3,6-disulfonate (M^{-1} s^{-1})
k_1 (protonation of RO^-)	$(16 \pm 1) \times 10^{10}$	$(7 \pm 0.5) \times 10^{10}$
k_3 (protonation of In^-)	$(4 \pm 0.2) \times 10^{10}$	$(4 \pm 0.2) \times 10^{10}$
k_5 (protonation of buffer)	$(2.8 \pm 0.2) \times 10^{10}$	$(2.0 \pm 0.1) \times 10^{10}$
k_7 (collisional proton exchange between indicator and buffer, favorable direction)	$(2 \pm 1) \times 10^9$	$(2 \pm 1) \times 10^9$
k_{10} (collisional proton exchange between buffer and RO^-, favorable direction)	$(2.5 \pm 0.5) \times 10^9$	$(1 \pm 0.2) \times 10^9$
k_{12} (collisional proton exchange between indicator and RO^-, favorable direction)	$\geq 7.5 \times 10^7$	$\geq 7.5 \times 10^7$

[a] Mean values ± standard error as calculated from experiments using 20 μM bromocresol green, 100 μM hydroxypyrenetrisulfonate, or 1 mM 2-naphtholdisulfonate and 0.25–4 mM imidazole at pH 5.7–7.0.

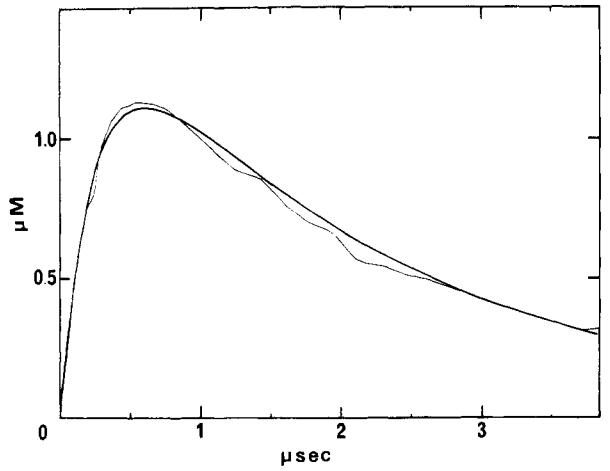

FIGURE 5: Experimental results and simulated curve for the dynamics of pulse protonation of bromocresol green in buffered solution. The reaction was measured in the presence of 1 mM 2-naphthol-3,6-disulfonate as proton emitter, 20 μM bromocresol green, and 250 μM imidazole, pH 7.0. The transient absorbance was measured with the 633-nm emission of the HeNe CW laser. The experiment represents the average of 512 events. The simulated curve employs the rate constants listed in Table I.

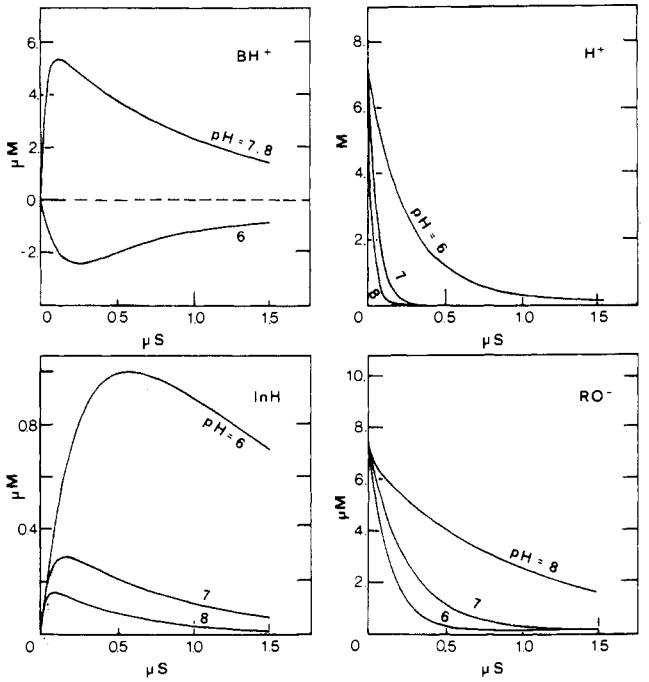

FIGURE 6: Computer simulation of the dynamics of all reactants participating in a laser-induced proton pulse in a buffered solution as taking place at pH 6, 7, and 8. The curves were generated for a solution containing 1 mM 2-naphthol-3,6-disulfonate, 20 μM bromocresol green, and 1.5 mM imidazole. (BH^+) The time-dependent variation of [H^+–imidazole]; (H^+) time-dependent variation of H^+; (InH) time-dependent variation of protonated indicator; (RO^-) time-dependent variation of sulfononaphtholate.

than that at pH 8, in spite of the fact that at pH 8 an appreciable fraction of ROH is deprotonated in its ground state. This faster relaxation at low pH demonstrates what a major role collisional proton transfer may have in buffered solutions.

The relaxation of free protons is obviously modulated by the buffer [Figure 6 (H^+)]. At pH 8, the protons are rapidly trapped by imidazole and only a few react with the indicator [Figure 6 (InH)]. At pH 6, the fraction of nonprotonated buffer is diminished, and the lifetime of the free proton is extended—accounting for the enhanced protonation of the indicator.

These results demonstrate how the buffer, supposedly an inert component, can modify the dynamics of the other reactants. In the accompanying paper (Gutman & Nachliel, 1985) we incorporate these concepts to analyze the effect of mobile and immobile buffer on proton flux between the surface of the macromolecular structure and the bulk of the bathing solution.

Appendix

The coupled differential equations describing the dynamics of a proton-pulse perturbation of a three-component system employ three time-dependent variables, X_t, Y_t and Z_t, which are the incremental dissociation of ROH and the incremental protonation of the indicator and buffer, respectively. The time-dependent concentration of free proton is given by

$$[H^+]_t = X_t - Y_t - Z_t$$

The rate constants appearing in the rate equations are defined in reactions 7–12.

The differential equations are

$$dX/dt = a_{11}X + a_{12}Y + a_{13}Z + b_{11}X^2 + b_{12}XY + b_{13}XZ$$

$$dY/dt = a_{21}X + a_{22}Y + a_{23}Z + c_{22}Y^2 + c_{12}XY + c_{23}YZ$$

$$dZ/dt = a_{31}X + a_{32}Y + a_{33}Z + d_{33}Z^2 + d_{13}XZ + d_{23}YZ$$

where the terms a_{ij}, b_{ij}, c_{ij}, and d_{ij} are defined as follows:

$$a_{11} = -k_1([H^+] + [RO^-]) - k_2 - k_{10}[BH] - k_9[B^-] - k_{12}[HIn] - k_{11}[In^-]$$

$$a_{12} = (k_1 - k_{12})[RO^-] - k_{11}[ROH]$$

$$a_{13} = (k_1 - k_{10})[RO^-] - k_9[ROH]$$

$$b_{11} = -k_1 \qquad b_{12} = k_1 - k_{12} + k_{11} \qquad b_{13} = k_1 + k_9 - k_{10}$$

$$a_{21} = (k_3 - k_{11})[In^-] - k_{12}[HIn]$$

$$a_{22} = -k_3([In^-] + [H^+]) - k_4 - k_8[BH] - k_7[B^-] - k_{11}[ROH] - k_{12}[RO^-]$$

$$a_{23} = (k_8 - k_3)[In^-] + k_7[HIn]$$

$$c_{22} = k_3 \qquad c_{12} = k_{11} - k_3 - k_{12} \qquad c_{23} = k_7 - k_8 + k_3$$

$$a_{31} = (k_5 - k_9)[B^-] - k_{10}[BH]$$

$$a_{32} = (k_7 - k_5)[B^-] + k_8[BH]$$

$$a_{33} = -k_5([B^-] + [H^+]) - k_6 - k_9[ROH] - k_{10}[RO^-] - k_7[HIn] - k_8[In^-]$$

$$d_{13} = k_9 - k_5 - k_{10} \qquad d_{23} = k_8 - k_7 + k_5 \qquad d_{33} = k_5$$

Registry No. 8-Hydroxypyrene-1,3,6-trisulfonate, 27928-00-3; 2-naphthol-3,6-disulfonate, 148-75-4; bromocresol green, 76-60-8; imidazole, 288-32-4; trisulfonopyrenate, 95911-56-1; sulfononaphtholate, 71576-14-2; bromocresol green anion, 47672-19-5.

References

Bennett, A. F., Buckley, P. D., & Blackwell, L. F. (1982) *Biochemistry 21*, 4407–4413.

Corin, A. F., Bersohn, R., & Cole, P. E. (1983) *Biochemistry 22*, 2032–2038.

Czerlinsky, G. H. (1966) *Chemical Relaxation*, Marcel Dekker, New York.

Eigen, M. (1964) *Angew. Chem., Int. Ed. Engl. 3*, 1–19.

Gutman, M. (1984) *Methods Biochem. Anal. 30*, 1–103.

Gutman, M., & Huppert, D. (1979) *J. Biochem. Biophys. Methods 1*, 19–29.

Gutman, M., & Nachliel, E. (1985) *Biochemistry* (following paper in this issue).
Gutman, M., Huppert, D., & Pines, E. (1981) *J. Am. Chem. Soc. 103*, 3709–3717.
Gutman, M., Nachliel, E., Gershon, E., & Giniger, R. (1983a) *Eur. J. Biochem. 134*, 63–69.
Gutman, M., Nachliel, E., Gershon, E., Giniger, R., & Pines, E. (1983b) *J. Am. Chem. Soc. 105*, 2210–2216.
June, D. S., Saelter, C. H., & Dye, J. L. (1981) *Biochemistry 20*, 2707–2719.
MacKnight, M. L., Gillard, J. M., & Tollin, G. (1973) *Biochemistry 12*, 4200–4206.
March, K. L., Maskalik, G. D., England, R. D., Friend, S. H., & Gurd, F. R. N. (1982) *Biochemistry 21*, 5241–5251.
Mathew, J. B., Hanania, G. I. H., & Gurd, F. R. N. (1981) *Biochemistry 20*, 571–580.
Nachliel, E., & Gutman, M. (1984) *Eur. J. Biochem. 143*, 83–89.
Shire, S. J., Hanania, G. I. H., & Gurd, F. R. N. (1974a) *Biochemistry 13*, 2967–2974.
Shire, S. J., Hanania, G. I. H., & Gurd, F. R. N. (1974b) *Biochemistry 13*, 2974–2979.
Shire, S. J., Hanania, G. I. H., & Gurd, F. R. N. (1975) *Biochemistry 14*, 1352–1358.
Silvestrini, M. C., Burnori, M., Wilson, M. T., & Darly-Usmar, V. M. (1981) *J. Inorg. Biochem. 14*, 327–338.
Tanford, C. (1976) *Physical Chemistry of Macromolecules*, Wiley, New York.

Kinetic Analysis of Protonation of a Specific Site on a Buffered Surface of a Macromolecular Body†

Menachem Gutman* and Esther Nachliel
Department of Biochemistry, Tel Aviv University, Tel Aviv, Israel
Received June 22, 1984; Revised Manuscript Received November 2, 1984

ABSTRACT: The kinetics of protonation of a specific site on a macromolecular structure (micelle) in buffered solution was studied with the purpose of evaluating the effect of buffer on the observed dynamics. The experimental system consisted of the following elements: Brij 58 micelles serving as homogeneous uncharged macromolecular bodies, bromocresol green, a well-adsorbed proton detector, and 2-naphthol-3,6-disulfonate as a proton emitter in the bulk. Imidazole was the mobile buffer while neutral red, which has a high affinity for the micellar surface, served as the immobile buffer. An intensive laser pulse ejects a proton from the proton emitter, and the subsequent proton-transfer reactions are measured by fast spectrophotometric methods. The dynamics of proton pulse in buffered solution are characterized by a very rapid trapping of the discharged protons by the abundant buffer molecules. This event has a major effect on the kinetic regime of the reaction. During the first 200 ns the proton flux is rate limited by free-proton diffusion. After this period, when the free-proton concentration decayed to the equilibrium level, the relaxation of the system is carried out by the diffusion of buffer. Thus in the buffered biochemical system, at neutral pH, most of proton flux between active sites and bulk is carried out by buffer molecules—not by diffusion of free protons. Surface groups on a high molecular weight body exchange protons among them at a very fast rate. This reaction has a major role on proton transfer from a specific site to the bulk. The proton can reach the bulk either through dissociation—diffusion or through collisional proton transfer between the mobile buffer and protonable surface groups. The rapid proton exchange between the surface groups increases the efficiency of the latter pathway. It is proposed that a combination of free proton diffusion and buffer-mediated proton diffusion can generate an apparent asymmetry in the "bulk to surface" vs. "surface to bulk" proton transfer. Low-pK surface groups will mostly enhance the rate of proton transfer from the bulk to a specific site on the surface, while basic groups on the surface will accelerate the dissipation of the proton to the bulk. This qualitative description is corroborated by accurate quantitative analysis based on experimentally determined rate constants.

There is hardly an enzyme-catalyzed reaction where the proton does not serve as a substrate, product, or intermediate. Thus, a rapid proton pulse can perturb most enzymic reactions through their interaction with the catalytic mechanism. Such perturbation is readily achieved by the laser-induced proton pulse (Gutman & Huppert, 1979), which can produce an intensive transinate acidification of aqueous solutions (10–50 μM H^+) within a few nanoseconds.

The application of this technique in enzymology is not straightforward due to the fact that the shape of the perturbing function is modulated by the reactants present in the solution (Gutman et al., 1983a,b; Gutman, 1984; Nachliel & Gutman, 1984). Because of that, any attempt to perturb the equilibrium of enzymes by a proton pulse and to measure the kinetics of the subsequent reaction will be hampered by the interaction of the protons with the rest of the proton binding sites in the solution (enzyme and substrate).

In the preceding paper (Gutman et al., 1985) we analyzed the effect of soluble buffer on the dynamics of protonation of a proton detector. In this paper we shall investigate the effect of buffer moieties carried by the same macromolecular body to which the proton detector is attached.

The model systems we selected for our studies are Brij 58 micelles carrying two pH indicators, bromocresol green and neutral red (Gutman et al., 1981; Nachliel & Gutman, 1984). In a previous study (Gutman et al., 1983b), we have measured the dynamics of protonation of each indicator when attached

† This research was supported by the American–Israel Binational Science Foundation, 3101/82.

0006-2960/85/0424-2941$01.50/0